British Journal of Pharmacology

DOI:10.1111/j.1476-5381.2012.02047.x
www.brjpharmacol.org

RESEARCH PAPER

Inhibition of human recombinant T-type calcium channels by *N*-arachidonoyl 5-HT

Andrew J Gilmore[1], Marika Heblinski[5], Aaron Reynolds[4], Michael Kassiou[2,3,4] and Mark Connor[2,5]

[1]*Pain Management Research Institute, Kolling Institute, University of Sydney at Royal North Hospital St Leonards,* [2]*Brain and Mind Research Institute, University of Sydney, Camperdown,* [3]*School of Chemistry, University of Sydney,* [4]*Discipline of Medical Radiation Sciences, University of Sydney, and* [5]*Australian School of Advanced Medicine, Macquarie University, Sydney, NSW, Australia*

Correspondence
Mark Connor, Australian School of Advanced Medicine, Macquarie University, Sydney, NSW 2109, Australia. E-mail: mark.connor@mq.edu.au

Keywords
T-type calcium channel; NA-5HT; NA-serotonin; anandamide; nociception; acyl amino acid; arachidonoyl amino acid

Received
23 November 2011
Revised
19 April 2012
Accepted
14 May 2012

BACKGROUND AND PURPOSE

N-arachidonoyl 5-HT (NA-5HT) has anti-nociceptive effects reported to be mediated by inhibitory actions at the transient receptor potential vanilloid receptor 1 (TRPV1) and fatty acid amide hydrolase (FAAH). Anandamide and *N*-arachidonoyl dopamine (NA-DA), endocannabinoids that activate TRPV1 or are metabolized by FAAH, also inhibit T-type calcium channels (I_{Ca}). T-type I_{Ca} are expressed by many excitable cells, including neurons involved in pain detection and processing. We sought to determine whether NA-5HT also modulates T-type I_{Ca}.

EXPERIMENTAL APPROACH

Human recombinant T-type I_{Ca} (Ca_V3 channels) expressed in HEK 293 cells were examined using standard whole-cell voltage-clamp electrophysiology techniques.

KEY RESULTS

NA-5HT completely inhibited Ca_V3 channels with a rank order of potency (pEC_{50}) of $Ca_V3.1$ (7.4) > $Ca_V3.3$ (6.8) ≥ $Ca_V3.2$ (6.6). The effects of NA-5HT were voltage-dependent, and it produced significant hyperpolarizing shifts in Ca_V3 steady-state inactivation relationships. NA-5HT selectively affected $Ca_V3.3$ channel kinetics.

CONCLUSIONS AND IMPLICATIONS

NA-5HT increases the steady-state inactivation of Ca_V3 channels, reducing the number of channels available to open during depolarization. These effects occur at NA-5HT concentrations at or below those at which NA-5HT affects TRPV1 receptors and FAAH. NA-5HT is one of the most potent inhibitors of T-type I_{Ca} described to date, and it is likely to exert some of its biological effects, including anti-nociception, via inhibition of these channels.

Abbreviations

FAAH, fatty acid amide hydrolase; GIRK, G-protein-gated inwardly rectifying K channels; I_{Ca}, voltage-gated calcium channel current; NA-5HT, N-arachidonoyl 5-HT; NAAN, *N*-acyl amino acid/neurotransmitters; NA-DA, *N*-arachidonoyl dopamine; NA-Gly, *N*-arachidonoyl glycine; TRPV1, transient receptor potential vanilloid receptor 1

Introduction

Fatty acids conjugated with amino acids or neurotransmitters (*N*-acyl amino acid/neurotransmitters, NAAN) are a class of endogenous compounds with a widespread tissue distribution and potential to modulate many aspects of cellular function (reviewed in Connor *et al.*, 2010). Several NAAN have been shown to have profound effects on nociception and inflammatory processes following local or systemic administration or incubation with tissue *in vitro* (Burstein *et al.*, 2000; Huang *et al.*, 2001; 2002; Succar *et al.*, 2007; Vuong *et al.*, 2008; Barbara *et al.*, 2009). These effects are likely to be

mediated via a range of molecular targets including cannabinoid CB_1 receptors (Bisogno *et al.*, 2000), transient receptor potential vanilloid 1 (TRPV1) receptors (Huang *et al.*, 2002), glycine transporters and receptors (Wiles *et al.*, 2006; Yang *et al.*, 2008) and T-type calcium channels (Ca_V3; Barbara *et al.*, 2009; Ross *et al.*, 2009). It is an open question whether tissue levels of any of these NAAN are high enough to effect these proteins (Marinelli *et al.*, 2007), but NAAN are becoming valuable pharmacological tools as both structurally novel ligands for existing modulatory sites and probes for new sites potentially amenable to pharmacological manipulation (Edington *et al.*, 2009; Yevenes and Zeilhofer, 2011).

Ca_V3 channels are expressed in many neurons involved in sensory processing, and knockout of $Ca_V3.1$ or $Ca_V3.2$ in mice has revealed deficits in the detection or processing of noxious stimuli sensory neurons in several brain regions (Kim *et al.*, 2003; Bourinet *et al.*, 2005; Park *et al.*, 2010). In contrast to the situation with high voltage-activated calcium channels (HVA I_{Ca}), there are few selective inhibitors of Ca_V3 channels available, which makes defining their function by means other than gene knockout difficult. Previous work has shown that NA-DA, NA-Gly and NA-GABA inhibit Ca_V3 channels in a manner similar to that of the prototypical endocannabinoid anandamide, although the fine details of channel modulation differ, indicating subtle differences in the interactions of these molecules with the putative binding site on the channels (Chemin *et al.*, 2001; 2007; Barbara *et al.*, 2009; Ross *et al.*, 2009). Interestingly, NA-DA and NA-Gly do not inhibit HVA I_{Ca} (Guo *et al.*, 2008). Together, these data suggest that the study of NAAN effects on Ca_V3 I_{Ca} may provide insight into the design of more specific modulators of these channels.

NA-5HT was one of the earliest NAAN synthesized (Bisogno *et al.*, 1998), but it was not until quite recently that it was found to occur *in vivo* (Verhoeckx *et al.*, 2011). NA-5HT is a very poor CB_1 receptor ligand, a relatively weak inhibitor of the anandamide degrading enzyme fatty acid amide hydrolase (FAAH), but a potent TRPV1 antagonist (Bisogno *et al.*, 1998; Fowler *et al.*, 2003; Maione *et al.*, 2007). These properties have been exploited to explore the potential contribution of the endocannabinoid system to the modulation of responses to nociception and inflammation in brain (Suplita *et al.*, 2005; de Novellis *et al.*, 2008; 2011), spinal cord (Suplita *et al.*, 2006) and the periphery (D'Argenio *et al.*, 2006; Costa *et al.*, 2010). While some of these studies show that the effects of NA-5HT are consistent with an increase of cannabinoid receptor-mediated effects of endocannabinoids secondary to inhibition of FAAH or via inhibition of TRPV1 activation, there are other actions of NA-5HT that are not easily ascribed to either of these mechanisms (D'Argenio *et al.*, 2006; Di Marzo *et al.*, 2008). Furthermore, cannabinoid receptor- and TRPV1-independent effects of NA-5HT on cancer cell growth (Jacobsson *et al.*, 2001; Bifulco *et al.*, 2004) have been reported. In light of these studies and our previous findings with NA-DA, we examined the actions of NA-5HT on T-type calcium channels. We find that NA-5HT is a potent inhibitor of Ca_V3 channel activity, particularly that of $Ca_V3.1$. These effects of NA-5HT on T-type channels are likely to contribute to the previously described effects of the compound in brain and cell lines and make NA-5HT the most potent endogenous modulator of T-type calcium channels identified to date.

Methods

Cell culture

HEK 293 cells stably transfected with plasmids containing cDNA for the human $Ca_V3.1$, $Ca_V3.2$ or $Ca_V3.3$ (Cribbs *et al.*, 1998; 2000; Gomora *et al.*, 2002; Ross *et al.*, 2008) were cultivated in DMEM supplemented with 100 U penicillin, 100 μg streptomycin, 10% FBS and 1 mg·mL^{-1} G418 (Invitrogen or Invivogen, Sydney, Australia). For some experiments, we used HEK 293 cells in which the same channels had been integrated into a FLP site under the control of a tetracycline repressor. In these experiments, channel expression was induced by overnight incubation with tetracycline (1 μg·mL^{-1}; Sigma, Sydney, Australia). AtT-20 cells stably expressing human $5\text{-}HT_{1B}$ receptors were grown as outlined above, except that the G418 concentration was 500 μg·mL^{-1} (Heblinski and Connor, 2012).

Electrophysiology

Calcium channel currents in HEK 293 cells were recorded in the whole-cell configuration of the patch-clamp method (Hamill *et al.*, 1981) at room temperature (Ross *et al.*, 2008). Dishes were perfused with HEPES-buffered saline (HBS) containing (in mM): 140 NaCl, 2.5 KCl, 2.5 $CaCl_2$, 1 $MgCl_2$. 10 HEPES, 10 Glucose (pH to 7.3, osmolarity = 330 ± 5 mosmol). For recording $Ca_V3.1$ and 3.2 currents, cells were bathed in an external solution containing (in mM): 140 tetraethylammonium chloride, 2.5 CsCl, 10 HEPES, 10 glucose, 1 $MgCl_2$, 5 $CaCl_2$ (pH to 7.3, osmolarity = 330 ± 5 mosmol). For recording $Ca_V3.3$ currents, 5 mM $CaCl_2$ was replaced by 5 mM $BaCl_2$ in the external solution (see Ross *et al.*, 2008) unless otherwise stated. Recordings were made with fire-polished borosilicate glass pipettes with resistance ranging from 2 to 3 MΩ. For recording $Ca_V3.1$ and 3.2 currents, the internal solution contained (in mM): 130 CsCl, 10 HEPES, 2 $CaCl_2$, 10 EGTA, 5 MgATP (pH to 7.3, osmolarity = 285 ± 5 mosmol). For recording of $Ca_V3.3$ currents, 10 mM EGTA was replaced by 10 mM BAPTA, and the concentration of MgATP was reduced to 1 mM. The different solutions used to record $Ca_V3.3$ were necessary to minimize current rundown (Ross *et al.*, 2008), although the reason(s) underlying this rundown in our cells are not established. Recordings were made with a HEKA EPC 10 amplifier with Patchmaster acquisition software (HEKA Elektronik, Germany) and an Axopatch 200B amplifier (Molecular Devices, Sunnyvale, CA) using AxoGraph X software (http://axographx.com/). Data were sampled at 5–20 kHz, filtered at 2 kHz, and recorded on hard disk for later analysis. Series resistance ranged from 3 to 10 MΩ and was compensated by at least 80% in all experiments. Leak subtraction using a P over 4 protocol (with 10 mV test steps) was used for a few of the experiments where cells were being stepped to a single potential, but it was not employed for experiments where more complex waveforms were applied to the cells (e.g. inactivation). Uncompensated leak in any experiment did not exceed –30 pA at –86 or –106 mV, and cells with a leak current of greater than –30 pA were discarded. Cells were exposed to drugs via flow pipes positioned approximately 200 μm from the cell. Concentration–response curves were generated by fitting data to a sigmoidal dose–response function in GraphPad

Prism 4 (http://www.graphpad.com/). Steady-state activation curves for $Ca_V3.1$ and 3.2 were generated from current–voltage relationships, while steady-state inactivation curves for each channel were generated by measuring the peak current from a 50 ms step to –26 mV following a series of 5 s steps ranging from potentials of –126 to –46 mV. Reported potentials are corrected for a junction potential of –6 mV. Activation curves were generated by fitting data to a Boltzmann sigmoidal function: $Y = 1 / (1 + e^{((V0.5 - Vm)/Slope)})$. Inactivation curves were generated by fitting data to a Boltzmann sigmoidal function: $Y = 1 - 1 / (1 + e^{((V0.5 - Vm)/Slope)})$.

$Ca_V3.3$ has unusual permeation properties and a relatively positive activation potential, which makes determining activation curves from chord conductances unreliable (Frazier *et al.*, 2001). Thus, we obtained activation curves for $Ca_V3.3$ channels by measuring the amplitude of tail currents at –90 mV following steps to positive potentials. The amplitude of the tail current is a direct measure of the number of open channels. To reduce the possible confounding effects of interactions in the pore of the channels between permeant monovalent and divalent cations, these experiments were carried out in solutions with only permeant monovalent ions. External solution for these experiments comprised (mM): NaCl 140, $MgCl_2$ 5, HEPES 10, TEACl 10; pH to 7.3, osmolarity = 330 ± 5 mosmol.

K currents in AtT-20 cells were recorded using an external solution comprising (mM): KCl 130, NaCl 35, $CaCl_2$ 1.5, HEPES 10, glucose 10, pH 7.3. The intracellular solution comprised (mM): KCl 130, NaCl 5, EGTA 10, $CaCl_2$ 2, HEPES 20, MgATP 5, NaGTP 0.2, pH 7.3. In some experiments, GDPβS or GTPγS (both 1.2 mM) was substituted for NaGTP. AtT-20 cells were voltage-clamped at –60 mV, and continuous recordings of current were made. In these conditions, opening of K channels produces an inward current.

NA-5HT synthesis

NA-5HT, (5*Z*,8*Z*,11*Z*,14*Z*)-*N*-(2-(5-hydroxy-1*H*-indol-2-yl) ethyl)icosa-5,8,11,14-tetraenamide, was synthesized as follows: triethylamine (32 µL, 0.23 mmol, 1.4 equiv) followed by *iso*-butylchloroformate (26 µL, 0.197 mmol, 1.2 equiv) was added to a stirred solution of arachidonic acid (54 µL, 0.16 mmol) in anhydrous acetonitrile (1 mL) at 0°C and under atmosphere of argon. The reaction mixture was stirred at 4°C for 40 min during which time a white precipitate formed. The solvent was evaporated under a stream of argon, and the residue obtained was treated with a solution of serotonin hydrochloride (38 mg, 0.197 mmol, 1.2 equiv) and triethylamine (25 µL, 0.181 mmol, 1.1 equiv) in anhydrous *N*,*N*-dimethylformamide (1.0 mL). The resultant pale yellow solution was stirred at 4°C for 18 h, after which time the reaction mixture was diluted with water and extracted with ethyl acetate. The organic extracts were combined, washed sequentially with water and brine, dried over anhydrous sodium sulfate and concentrated *in vacuo*. The crude residue obtained was purified by flash chromatography on silica gel, eluting with hexaneethyl acetate (1:1), to produce (5*Z*,8*Z*,11*Z*,14*Z*)-*N*-(2-(5-hydroxy-1*H*-indol-2-yl)ethyl)icosa-5,8,11,14-tetraenamide (71 mg, 93%) as a colourless gum.

^1H and ^{13}C NMR spectra were acquired at 300 ± 1 K using either a Bruker DP X400 (400 MHz). ^1H chemical shifts are reported relative to residual non-deuterated solvent resonance or tetramethylsilane. Low-resolution mass spectra were recorded on a Finnigan LCQ mass spectrometer. High-resolution mass spectra were recorded by the Mass Spectrometry Unit of the School of Chemistry, University of New South Wales. Structural information was as follows: ^{1}H NMR (400.2 MHz, CDCl3) δ 7.21 (1H, d, *J* = 8.8 Hz), 7.00 (1H, dd, *J* = 17.8, 2.2 Hz), 6.80 (1H, dd, *J* = 8.8, 2.4 Hz), 5.58–5.30 (10H, br m), 3.57 (2H, dd, *J* = 12.8, 6.8 Hz), 2.89 (2H, t, *J* = 6.8 Hz), 2.84–2.76 (6H, m), 2.13 (2H, t, *J* = 7.6 Hz), 2.10–2.02 (4H, m), 1.72–1.64 (4H, m), 1.39–1.23 (6H, m), 0.88 (3H, t, *J* = 6.8 Hz); ^{13}C NMR (100.6 MHz, $CDCl_3$) δ 173.1, 149.9, 131.6, 130.6, 129.2, 128.7, 128.6, 128.2, 128.2, 128.1, 127.9, 127.5, 123.0, 112.4, 112.2, 111.9, 130.3, 39.7, 36.2, 31.5, 29.3, 27.2, 26.7, 25.6, 25.5, 25.5, 22.6, 14.1; MS (+ESI) *m*/*z* 485 ($[M + Na]_+$, 28%), 947 ($[2 M + Na]_+$, 100); HRMS (+ESI) calculated for $C_{30}H_{42}N_2O_2$ ($[M + Na]_+$) 485.31385, found 485.31381.

Pharmacological agents. NA-5HT was either obtained from Alexis Biochemicals (Lausen, Switzerland), Biomol (Plymouth Meeting, PA), Cayman Chemical (Ann Arbor, MI) or synthesized by us. Results were similar with drugs purchased from all sources. Oleoyl- and palmitoyl-5HT were from Cayman Chemical. Arachidonic acid for synthesis was from Biomol. All other drugs and chemicals were from Sigma Australia.

Drug vehicle (ethanol). Drugs were kept in concentrated stock solutions in ethanol and stored at –30°C. Daily dilutions from these stocks were made; the final ethanol concentration in all solutions was 0.1%. Ethanol at this concentration does not significantly affect the properties of the Ca_V3 channels (Ross *et al.*, 2009).

Statistics

Statistical significance for comparing the $V_{0.5}$ values of activation and inactivation was determined using Student's unpaired *t*-test comparing values of $V_{0.5}$ calculated for individual experiments. In order to compare the changes in the time constants of inactivation and deactivation, a two-way ANOVA test was used with a Bonferroni post test to compare values at different potentials.

Drug and molecular target nomenclature conforms to the *BJP Guide to Receptors and Channels* (Alexander *et al.*, 2011).

Results

NA-5HT inhibited each of the human Ca_V3 subtypes (Figure 1). The inhibitory effects of NA-5HT on Ca_V3 channels developed relatively slowly and did not readily reverse on washing. However, a substantial reversal of NA-5HT (300 nM) inhibition of $Ca_V3.1$ could be achieved by inclusion of BSA (1%) in the wash buffer (Figure 2). BSA itself had no effect on $Ca_V3.1$ current amplitude (Figure 2; current was 109 ± 2% of initial after 10 min in BSA, *n* = 6). The potency of NA-5HT inhibition of Ca_V3 channels was determined by superfusing single concentrations of drug onto cells repetitively stepped from –86 to –26 mV. NA-5HT inhibited $Ca_V3.1$ with pEC_{50} of 7.36 ± 0.09 (~40 nM), $Ca_V3.2$ with a pEC_{50} of 6.59 ± 0.15 (~250 nM) and $Ca_V3.3$ with a pEC_{50} of 6.79 ± 0.06 (~160 nM) (Figure 3). *N*-oleoyl 5-HT (18:1ω9, 10 µM) inhibited Ca_V3

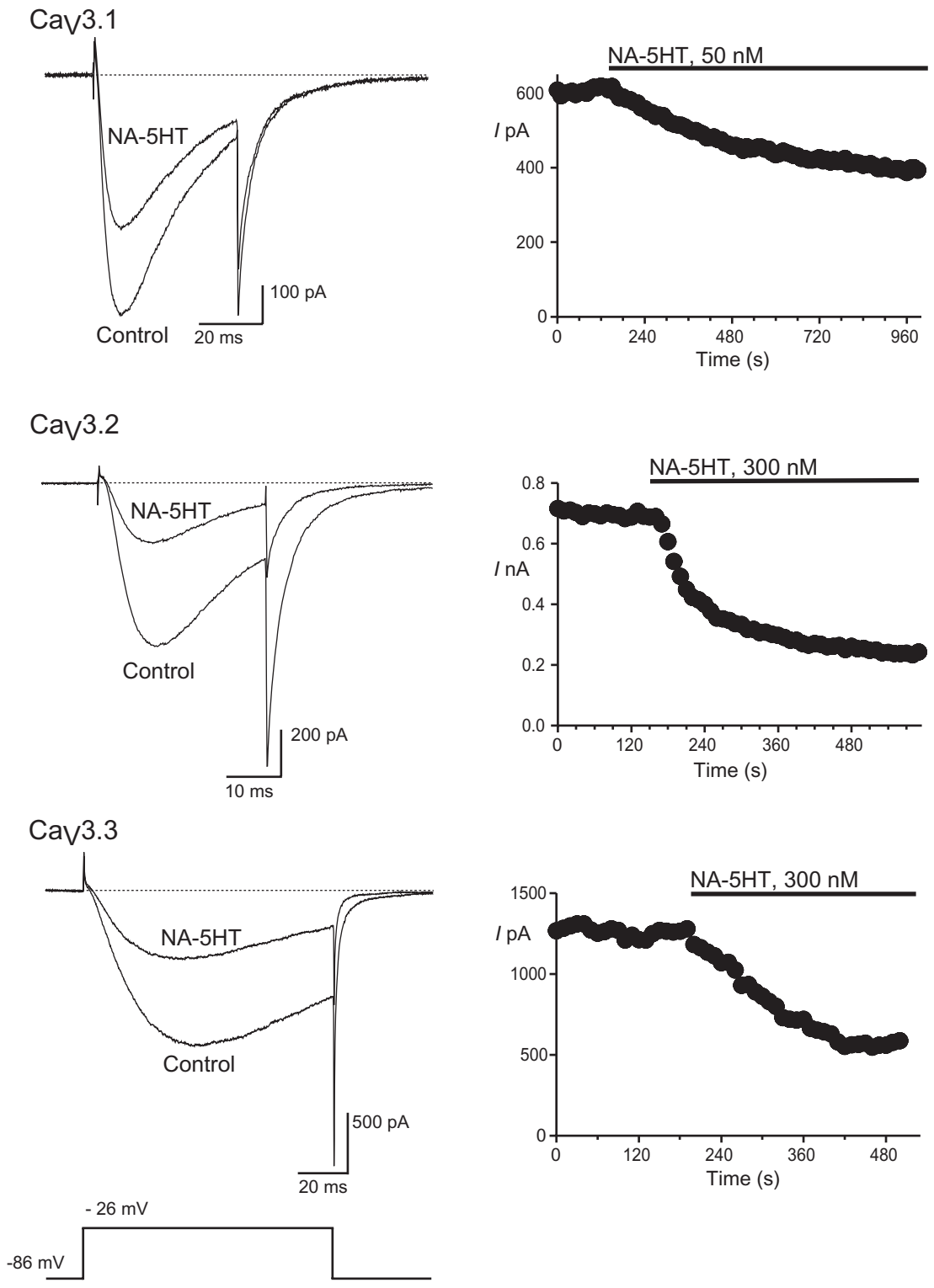

Figure 1

N-arachidonoyl 5-HT inhibits recombinant human T-type calcium channels. Whole-cell patch clamp recordings were made from human $Ca_v3.1$, $Ca_v3.2$ and $Ca_v3.3$ channels stably expressed in HEK 293 cells. Currents were evoked by stepping from –86 to –26 mV every 10 s. The effect of NA-5HT on each of $Ca_v3.1$, $Ca_v3.2$ and $Ca_v3.3$ are illustrated, with a representative time plot and example traces. Each trace is an example of at least six similar experiments. NA-5HT was applied for the duration of the bar. The dotted line represents zero current.

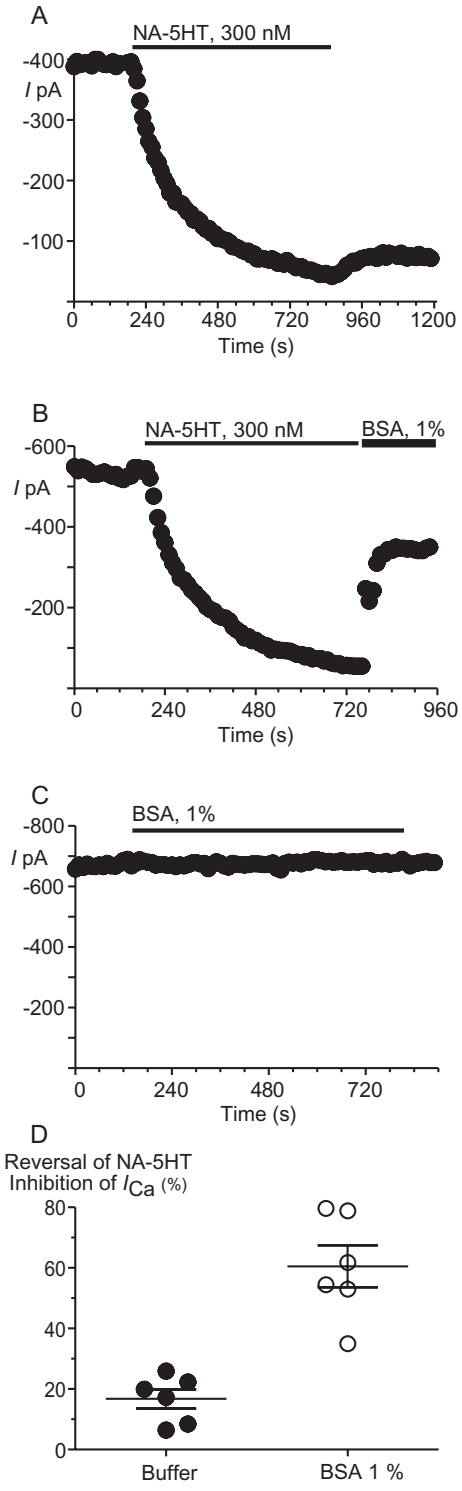

Figure 2

N-arachidonoyl 5HT inhibition of $Ca_V3.1$ is reversed by BSA. Whole-cell patch clamp recordings were made from human $Ca_V3.1$ HEK 293 cells. Currents were evoked by stepping from –86 to –26 mV every 10 s. Representative time plots of the effect of washing off *N*-arachidonoyl 5-HT with (A) buffer alone and (B) BSA are illustrated. (C) BSA alone had no effect on $Ca_V3.1$ currents. BSA significantly ($P < 0.001$, Student's *t*-test) enhanced the reversal of NA-5HT inhibition of $Ca_V3.1$, summarized in (D). The bars represent the mean ± SEM.

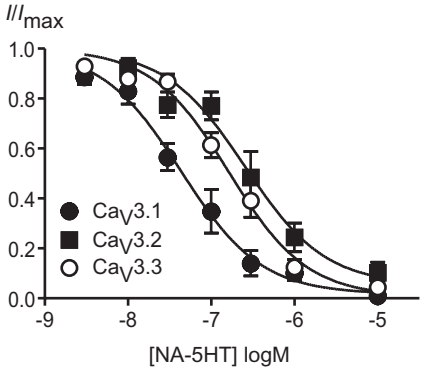

Figure 3

Concentration–response plot for *N*-arachidonoyl 5-HT inhibition of Ca_V3 channels. Whole-cell patch clamp recordings were made from human $Ca_V3.1$, $Ca_V3.2$ and $Ca_V3.3$ channels stably expressed in HEK 293 cells. Currents were evoked by stepping from –86 to –26 mV every 10 s. A single concentration of drug was superfused over each cell. Each point represents the mean ± SEM of at least six cells. NA-5HT inhibits Ca_V3 channels with a rank order of $Ca_V3.1$ (50 nM) > $Ca_V3.3$ (200 nM) > $Ca_V3.2$ (250 nM).

channels to similar degree as NA-5HT (10 μM), but the unsaturated *N*-palmitoyl 5-HT (C16, 10 μM) was much less effective (Figure 4).

NA-5HT effect on channel activation and inactivation

Arachidonic acid and its conjugates inhibit Ca_V3 channels in part by increasing steady-state inactivation and thus reducing the numbers of channels available to open during a depolarization. We examined whether the inhibition of Ca_V3 channels by NA-5HT could be due to effects on channel availability or activation (Figure 5). For $Ca_V3.1$ and 3.2, activation curves were constructed by stepping cells from –106 mV to potentials between –86 and +59 mV, and then were repeated after 5 min perfusion of submaximally effective concentrations of NA-5HT. In the presence of NA-5HT, there were small (2–3 mV) shifts in the potential at which half the channels were activated; these shifts were not different from those seen with time-matched vehicle controls (Figure 5, Table 1). The voltage-dependence of activation for $Ca_V3.3$ was determined by measuring tail currents at –90 mV immediately following steps to positive voltages (see Methods). The $V_{0.5}$ for activation of $Ca_V3.3$ was not different from pre-drug in the presence of NA-5HT (300 nM); however, the small time-dependent shift in $V_{0.5}$ seen in parallel control experiments (~2 mV) was not observed in the presence of NA-5HT (Figure 5, Table 1).

Steady-state inactivation was determined by holding cells at –106 mV and then stepping them for 5 s to test potentials between –126 and –51 mV before measuring the current following a step to –26 mV. This was repeated after 5 min in submaximal inhibitory concentrations of drug. NA-5HT produced a significant hyperpolarizing shift in the membrane potential at which 50% of the channels were available for activation for each channel (Figure 5, Table 1). The shifts in steady-state inactivation in cells exposed to vehicle alone for

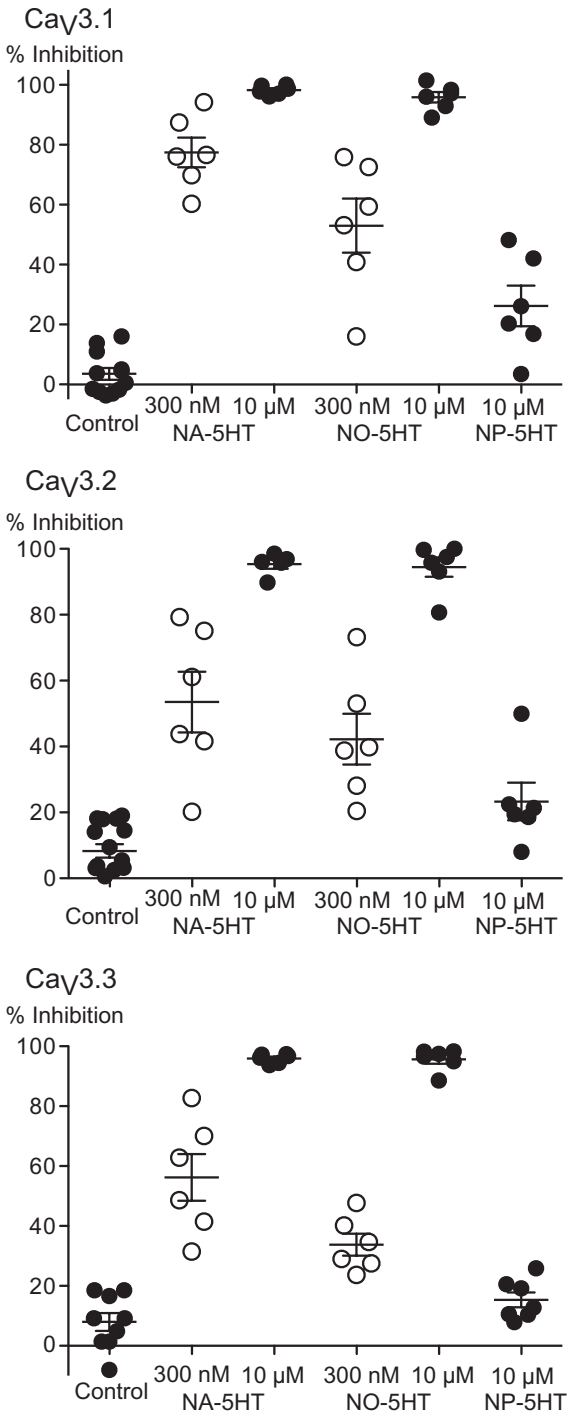

Figure 4

Unsaturated *N*-acyl 5-HT analogues inhibit recombinant human T-type calcium channels more effectively than the saturated NP-5HT. Whole-cell patch clamp recordings were made from human $Ca_V3.1$, $Ca_V3.2$ and $Ca_V3.3$ channels stably expressed in HEK 293 cells. Currents were evoked by stepping from –86 to –26 mV every 10 s. A summary of the effect of 300 nM and 10 μM *N*-arachidonoyl 5-HT (NA-5HT), *N*-oleoyl 5-HT (NO-5HT) and 10 μM *N*-palmitoyl 5-HT (NP-5HT) on each of $Ca_V3.1$, $Ca_V3.2$ and $Ca_V3.3$ is illustrated. The bars are the mean ± SEM of five to seven cells for each drug on each channel. Control experiments for each represent superfusion of vehicle alone.

5 min were less than 2 mV (Table 1). The increase in steady-state inactivation is likely to make a major contribution to the inhibition of Ca_V3 channel currents by NA-5HT.

If the effects of NA-5HT on channel inactivation contributed significantly to the inhibition of the Ca_V currents, then applying NA-5HT to cells voltage-clamped at potentials significantly more negative than –86 mV would be expected to produce less inhibition of channel currents. The inhibition by 50 nM NA-5HT of $Ca_V3.1$ currents elicited by a step to –26 mV was significantly less when cells were held at –106 mV (20 ± 7%, P = 0.007) or –126 mV (25 ± 7%, P = 0.014) than when they were held at –86 mV (55 ± 8% n = 6–7 for each).

The effects of NA-5HT on Ca_V3 channels were not significantly affected when GTP was omitted from the pipette (Figure 6), implying a lack of G-protein involvement in the channel inhibition. We further tested this by examining the effects of NA-5HT on $Ca_V3.1$ when the competitive inhibitor of G-protein activation, GDPβS (1.2 mM) or the irreversible activator of G-proteins GTPγS (1.2 mM) was included in the pipette. In the presence of internal GTPγS, inhibition of $Ca_V3.1$ by 50 nM NA-5HT was 61 ± 8% compared with 64 ± 4% in cells with GTP-containing internal (n = 6 for each). In a separate set of experiments, the inhibition of $Ca_V3.1$ by 50 nM NA-5HT was 38 ± 8% in the presence of GDPβS and 51 ± 12% in GTP (n = 6 for each). Neither nucleotide derivative significantly affected the inhibition of $Ca_V3.1$ channels by NA-5HT. In control experiments, GDPβS strongly reduced $5HT_{1B}$ receptor-mediated activation of G-protein-gated inwardly rectifying K channels (GIRK) in AtT-20 cells. Current produced by application of 100 nM 5HT was –180 ± 10 pA in control and –13 ± 3 pA in the presence of GDPβS (n = 4). Conversely, addition of GTPγS to the internal solution produced a rapidly developing spontaneous inward current that peaked at –330 ± 130 pA (n = 5). This current occluded the effect of any subsequent application of 5HT.

We examined the effects of NA-5HT on Ca_V3 channel kinetics by comparing the effects of 5 min applications of compound with time-matched controls. Currents were elicited from a holding potential of –106 mV, and we measured the time to peak and time constant of channel inactivation from an open state. Because the voltage steps were long enough to capture most of the channel inactivation, tail currents on re-polarization were very small, so channel deactivation was examined in a separate series of experiments (see below). NA-5HT did not affect time to peak or inactivation from an open state for $Ca_V3.1$ (50 nM) or $Ca_V3.2$ (300 nM) (Figure 7). However, NA-5HT (300 nM) significantly accelerated both the time to peak and rate of inactivation from an open state for $Ca_V3.3$ over a wide range of test potentials (Figure 8, ANOVA). In a separate series of experiments where we examined the activation of $Ca_V3.3$ using only permeant monovalent cations (see above), the time to peak for the currents was also significantly accelerated. The time to peak for a step from –90 to 0 mV was 23.4 ± 0.7 ms; after 5 min in 300 nM NA-5HT, it was 20.0 ± 0.5 ms (P = 0.0001, paired t-test, n = 7). In parallel control experiments, the time to peak was 20.4 ± 1.2 ms; 5 min later, it was 19.4 ± 0.9 ms (P = 0.18, paired t-test, n = 7).

The effects of NA-5HT on accelerating the activation kinetics of $Ca_V3.3$ were concentration-dependent. We ana-

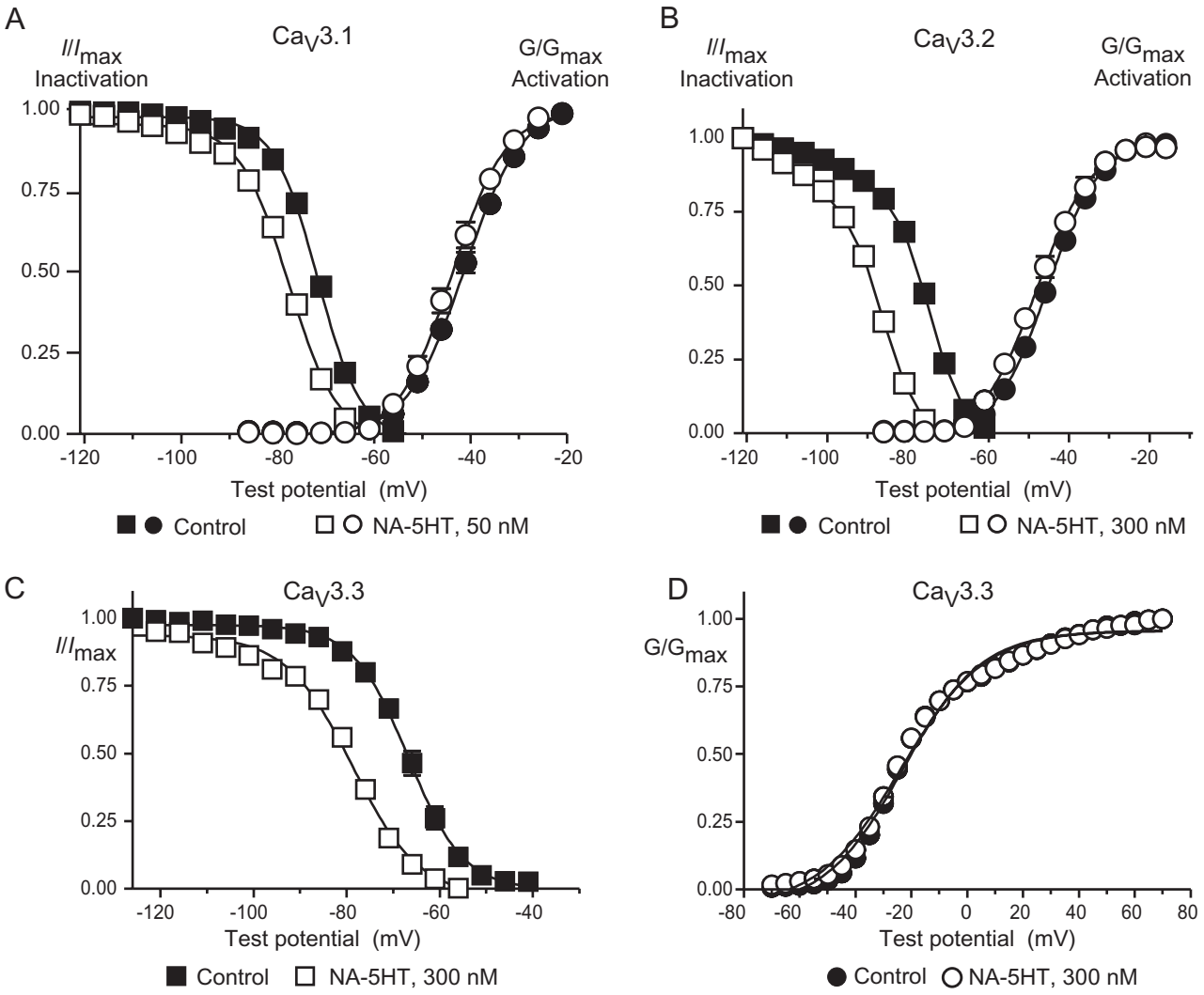

Figure 5

N-arachidonoyl 5-HT affects steady state inactivation but not activation of Ca_V3 channels. Whole-cell patch clamp recordings were made from human Ca_V3 channels stably expressed in HEK 293 cells, 5 min after breaking into the cell and then again after 5 min in NA-5HT. To measure channel activation, cells expressing $Ca_V3.1$ and $Ca_V3.2$ were voltage-clamped at –106 mV and stepped to potentials above –86 mV in 5 mV increments. The peak current at each test potential is plotted for $Ca_V3.1$ and $Ca_V3.2$ (A, B). Cells expressing $Ca_V3.3$ were voltage-clamped at –106 mV, stepped briefly to potentials between –86 and +74 mV and stepped back to –106 mV (see Methods). The amplitude of the tail current was plotted for $Ca_V3.3$ (D). To measure steady-state inactivation, cells were voltage-clamped for 5 s at potentials between –126 and –46 mV, and then stepped to a test potential of 26 mV. The current at –26 mV following 5 s at the indicated holding potential is plotted for inactivation. Curves are a Boltzmann fit of the data (see Methods). NA-5HT did not affect the voltage-dependence of channel activation but produced a significant hyperpolarizing shift in the membrane at which 50% of the channels are inactivated for each Ca_V3 subtype (A, B, C; Table 1).

lysed the time to peak of the $Ca_V3.3$ recordings used to generate the concentration-response curves described above. Currents were evoked from a holding potential of –86 mV to a test potential of –26 mV. Significant acceleration of channel activation was apparent at 1 μM NA-5HT ($P < 0.001$, *t*-test vs. parallel controls; Figure 9); by contrast, significant inhibition of the $Ca_V3.3$ current was apparent at concentrations of NA-5HT greater than 100 nM. We determined the effects of 1 μM NA-5HT on the time to peak of $Ca_V3.1$ and $Ca_V3.2$ using the same voltage protocol, with measurements made either at a steady-state inhibition (if inhibition was less than 90%) or when inhibition of the current was at approximately 90%, in cells where 1 μM NA-5HT produced a greater than 90% inhibition. We found that in contrast to the effects seen on $Ca_V3.3$ currents, NA-5HT did not affect the time to peak for either $Ca_V3.1$ or $Ca_V3.2$ (Figure 9).

We examined the effects of NA-5HT (1 μM) on tail currents resulting from re-polarization of cells from –26 to –86 mV. The tail currents were best fit by a two-component exponential. Data were collected from time points where the currents were maximally inhibited or inhibited by about 90% of control, whichever was the larger current. NA-5HT did not significantly affect any of the kinetic parameters of the $Ca_V3.1$ or $Ca_V3.2$ tail currents (n = 6–8, paired *t*-test; Figure 10).

Table 1

The effects of NA-5HT on the parameters of steady-state activation and inaction of Ca_V3 channels

Drug	CaV	Change in $V_{0.5}$ (mV) Activation	Inactivation
50 nM NA-5HT	3.1	−3 ± 1	−7 ± 1**
300 nM NA-5HT	3.2	0 ± 1	−12 ± 1**
300 nM NA-5HT	3.3	−0.5 ± 0.2	−12 ± 0.5**
No drug	3.1	−2 ± 1	−1.5 ± 0.4
No drug	3.2	1 ± 2	−3 ± 1
No drug	3.3	−2 ± 1	−2 ± 0.5

Cells expressing recombinant Ca_V3 channels were voltage-clamped at −106 mV and then stepped to potentials above −86 mV (activation) or stepped for 5 s to potentials between −126 and −36 mV before stepping to the test potential of −26 mV. $Ca_V3.3$ activation curves were determined from tail current analysis, as outlined in the Methods. The resulting peak currents were fitted to a Boltzmann equation. Changes in the voltage for half activation/inactivation ($V_{0.5}$) of the curves are reported below. No drug represents time-dependent changes under our recording conditions. Data are illustrated in Figure 5. **$P < 0.001$ from control.

However, in the presence of 1 μM NA-5HT, the major component of the $Ca_V3.3$ channel deactivation was significantly accelerated, from 1.83 ± 0.30 to 1.29 ± 0.28 ms ($P < 0.001$, paired *t*-test, $n = 7$; Figure 10). The proportion of the tail current accounted for by this component did not change (0.80 ± 0.02 in control, 0.76 ± 0.04 in drug), and there was no significant change in the properties of the minor component of the tail current. There were no changes in the kinetics of the tail currents of time-matched control recordings.

Discussion

The major finding of this study is that NA-5HT inhibits T-type calcium channels with a similar potency to its antagonist actions at native TRPV1 receptors and with a much greater potency than its inhibitory actions at FAAH. Thus, inhibition of T-type calcium channels, which have a well-established role in neuronal activity related to nociception in both the central and peripheral nervous system (Shin *et al.*, 2008), is likely to mediate at least some of the anti-nociceptive effects of NA-5HT.

The EC_{50} of NA-5HT to inhibit $Ca_V3.1$ under our experimental conditions is about 50 nM, which compares favourably with compounds being developed by the pharmaceutical industry as T-type calcium channel inhibitors (Giordanetto *et al.*, 2011). NA-5HT is the most potent fatty acid-derived inhibitor of $Ca_V3.1$ and $Ca_V3.3$ identified (Chemin *et al.*, 2001; Barbara *et al.*, 2009; Ross *et al.*, 2009). NA-5HT also inhibited $Ca_V3.2$ (EC_{50} = 250 nM) at concentrations similar to *N*-arachidonoyl GABA hydroxide (NA-GABA-OH), the most potent NAAN previously examined (EC_{50} = 200 nM; Barbara *et al.*, 2009). Given the voltage-dependence of NA-5HT's

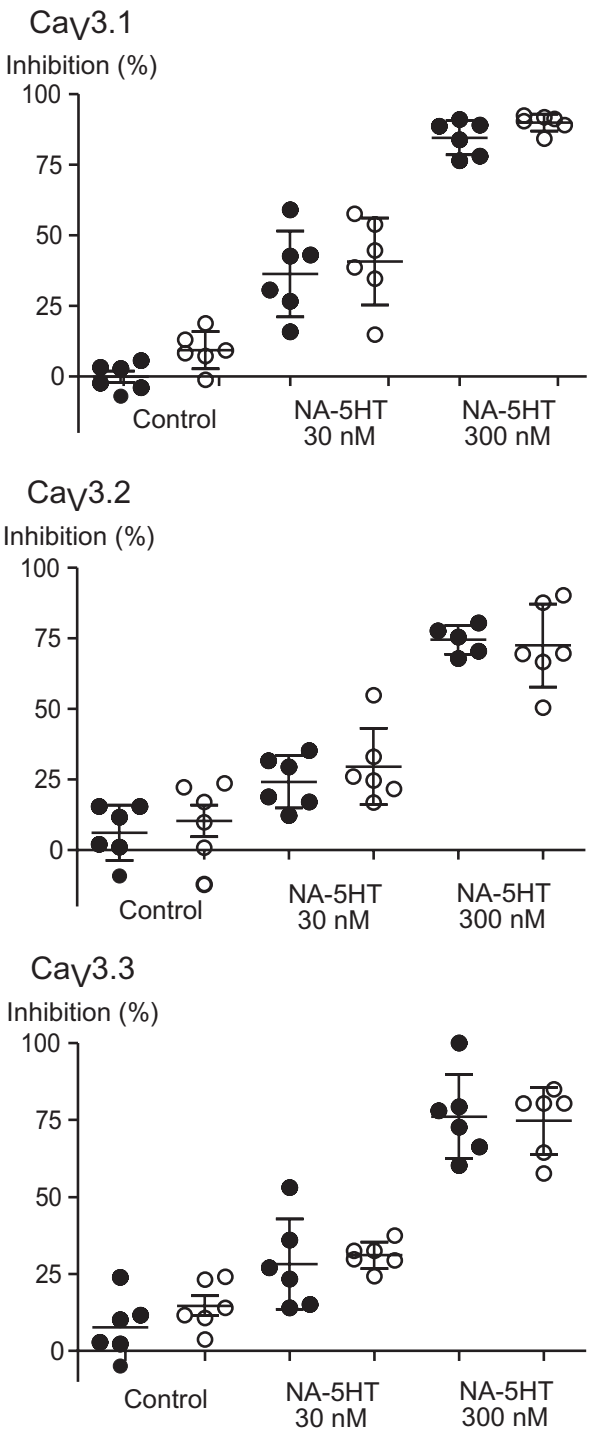

Figure 6

The effect of omission of GTP from the pipette solution on inhibition of Ca_V3 channels by *N*-arachidonoyl 5-HT. Whole-cell patch clamp recordings were made from human Ca_V3 channels stably expressed in HEK 293 cells with an internal solution that did or did not contain 0.3 mM GTP. Currents were evoked by stepping from −86 to −26 mV every 10 s. For each channel type, NA-5HT was superfused at low (30 nM) or high (300 nM) concentrations. Omission of GTP had no discernable effect on the NA-5HT inhibition of Ca_V3 channels. The bars are the mean ± SEM of six cells for each condition. Control experiments for each represent superfusion of vehicle alone.

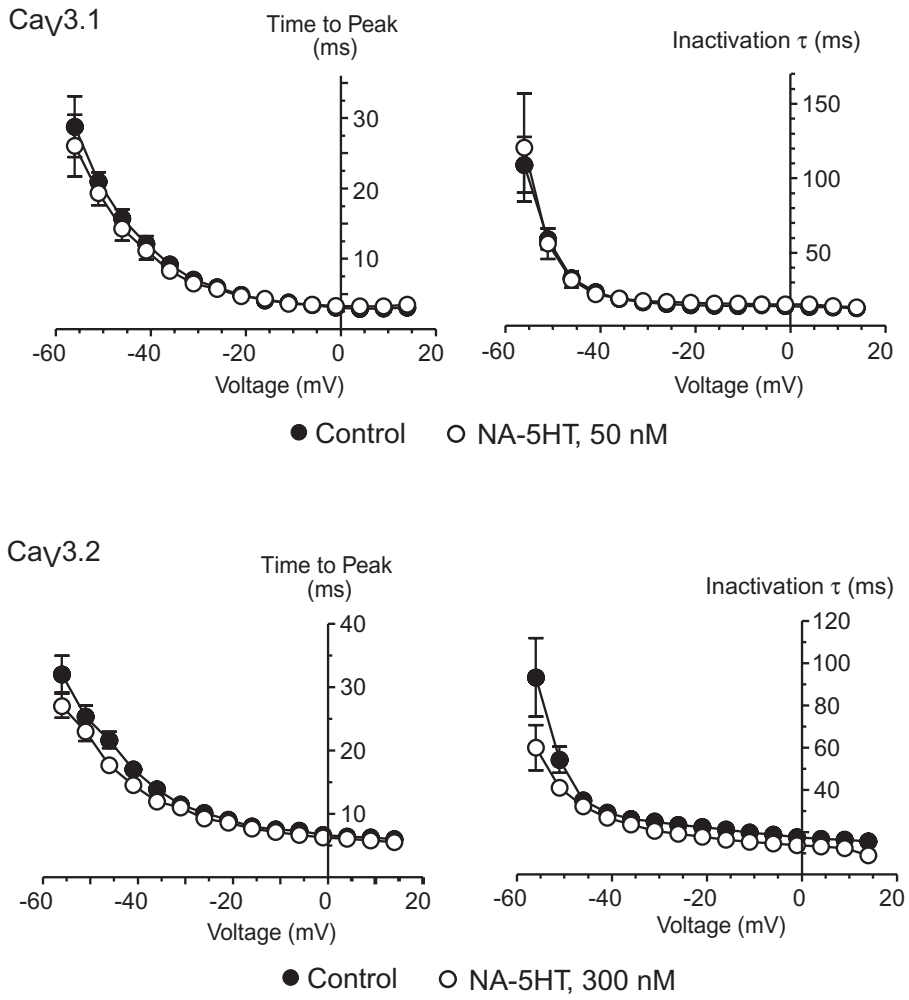

Figure 7

N-arachidonoyl 5-HT does not affect $Ca_V3.1$ or $Ca_V3.2$ channel kinetics. Whole-cell patch clamp recordings were made from human Ca_V3 channels stably expressed in HEK 293 cells. Channel activation and inactivation from the open state was measured by stepping cells from a holding potential of –106 mV to potentials above –86 mV. Currents were measured 5 min after breaking into the cell and then again after 5 min in NA-5HT. The plots illustrate the time to peak and time constant of current decline after peak before and after 5 min in NA-5HT. The small shifts seen were not different to those seen in parallel experiments where solvent alone was superfused. Each point represents the mean ± SEM of at least six cells.

actions, its effects at more depolarized membrane potentials are likely to be enhanced, as previously demonstrated for other lipophilic modulators of these channels (Chemin *et al.*, 2001; Ross *et al.*, 2008). The other major pharmacological targets of NA-5HT identified to date are TRPV1 and FAAH. NA-5HT inhibits capsaicin or anandamide activation of TRPV1 with an EC_{50} between 40 and 100 nM (Maione *et al.*, 2007), while inhibition of FAAH activity occurs with EC_{50} values between 1 and 10 μM (Bisogno *et al.*, 1998; Jonsson *et al.*, 2001; Fowler *et al.*, 2003). Given that inhibition of FAAH is likely to modulate the concentration of anandamide and related compounds that are ligands for both TRPV1 and Ca_V3 channels, the overall effects of endogenous or exogenously applied NA-5HT are likely to be complex. Delineating which effects of NA-5HT are mediated directly on target channels and which occur secondary to inhibition of FAAH will require careful experimental design. It is, however, unlikely that NA-5HT was inhibiting Ca_V3 I_{Ca} secondary to inhibition of FAAH and generation of AEA in our experiments. First, the concentrations of NA-5HT needed to inhibit each channel were at least 5- to 20-fold lower than those reported to inhibit FAAH (Bisogno *et al.*, 1998; Jonsson *et al.*, 2001; Fowler *et al.*, 2003). More pertinently, the characteristics of NA-5HT inhibition differ significantly from those of AEA, with NA-5HT only significantly affecting $Ca_V3.3$ channel kinetics, which is in contrast to the effects of AEA on the channel opening and open state inactivation (Chemin *et al.*, 2001; Ross *et al.*, 2009) of all Ca_V3 types, particularly $Ca_V3.1$. 2-Acyl glycerol, which may also be metabolized by FAAH, does not inhibit Ca_V3 channels (Chemin *et al.*, 2001).

T-type calcium channels are involved in a wide range of physiological processes (Perez-Reyes, 2003; Shin *et al.*, 2008), including many that are also potentially affected by the elevated levels of endocannabinoids resulting from NA-5HT inhibition of FAAH or NA-5HT inhibition of TRPV1. In particular, $Ca_V3.1$ channels have been reported to have an

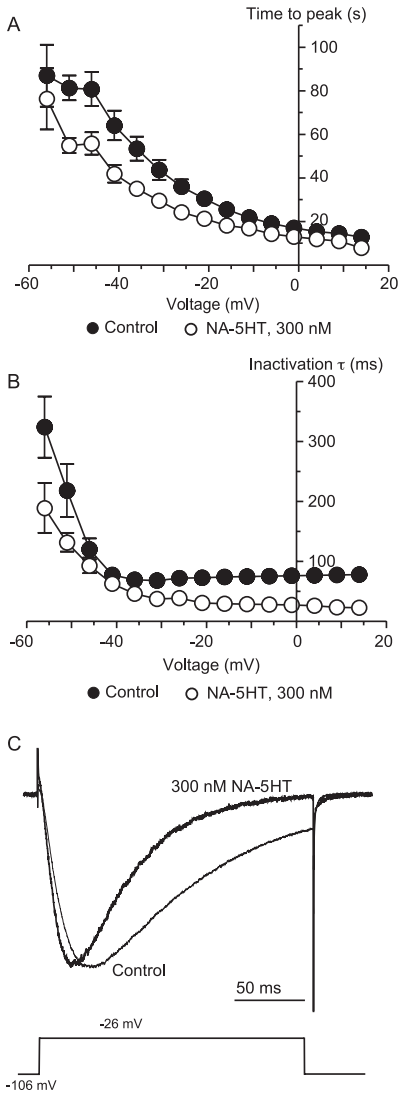

Figure 8

N-arachidonoyl 5-HT affects $Ca_V3.3$ channel kinetics. Whole-cell patch clamp recordings were made from human $Ca_V3.3$ channels stably expressed in HEK 293 cells. Channel activation and inactivation from the open state was measured by stepping cells from a holding potential of –106 mV to potentials above –86 mV. Currents were measured 5 min after breaking into the cell and then again after 5 min in NA-5HT (300 nM). The plots illustrate (A) the time to peak and (B) time constant (τ) of current decline after peak before and after 5 min in NA-5HT. Each point represents the mean ± SEM of at least six cells. NA-5HT accelerated channel activation and inactivation ($P < 0.05$, ANOVA). (C) Example trace of currents before and in the presence of NA-5HT, normalized to the peak current for each.

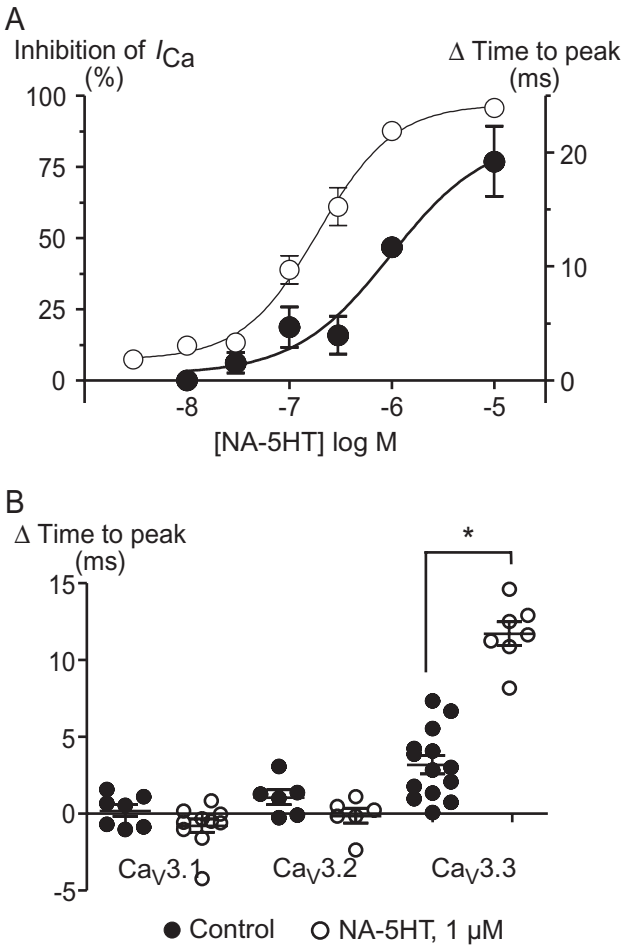

Figure 9

N-arachidonoyl 5-HT selectively affects $Ca_V3.3$ channel activation. Whole-cell patch clamp recordings were made from human $Ca_V3.1$, $Ca_V3.2$ and $Ca_V3.3$ channels stably expressed in HEK 293 cells. Currents were evoked by stepping cells repetitively from –86 to –26 mV every 10 s and time to peak determined in Axograph. Each point represents the mean ± SEM of at least six cells. (A) Illustrates the comparative potency of NA-5HT inhibition of $Ca_V3.3$ currents with its effects on channel time to peak. (B) Even at a high concentration (1 μM), NA-5HT selectively affects the time to peak of $Ca_V3.3$ but not $Ca_V3.1$ or $Ca_V3.2$. The bars are the mean ± SEM of at least six cells per condition. Control experiments represent superfusion of vehicle alone. *$P < 0.05$, Student's *t*-test.

important role in neurons involved in the endogenous anti-nociceptive circuits originating in the periaqueductal grey (Park *et al.*, 2010), a region where NA-5HT administration potentiates endogenous anti-nociception effects (Suplita *et al.*, 2005). However, demonstrating the relative contribution of T-type calcium channels compared with potential targets of NA-5HT, such as TRPV1 and FAAH, is further complicated because other drugs used to probe these mechanisms are themselves T-type I_{Ca} blockers; for example, the CB_1 receptor antagonists SR 141716A (Chemin *et al.*, 2001) and AM251 (Ross *et al.*, 2008) and the TRPV1 antagonist capsazepine (Docherty *et al.*, 1997) all inhibit native or recombinant T-type channels.

Intriguingly, NA-5HT inhibits the proliferation of C6 glioma cells (Jacobsson *et al.*, 2001) via mechanism(s) not involving CB_1 receptors or TRPV1 and also slows growth of K-ras-transformed rat thyroid cells by a CB_1-independent process (Bifulco *et al.*, 2004). There is a strong correlation between the expression of T-type calcium channels and growth in some cancer cells and inhibition of these channels slows growth significantly (reviewed in Panner and Wurster,

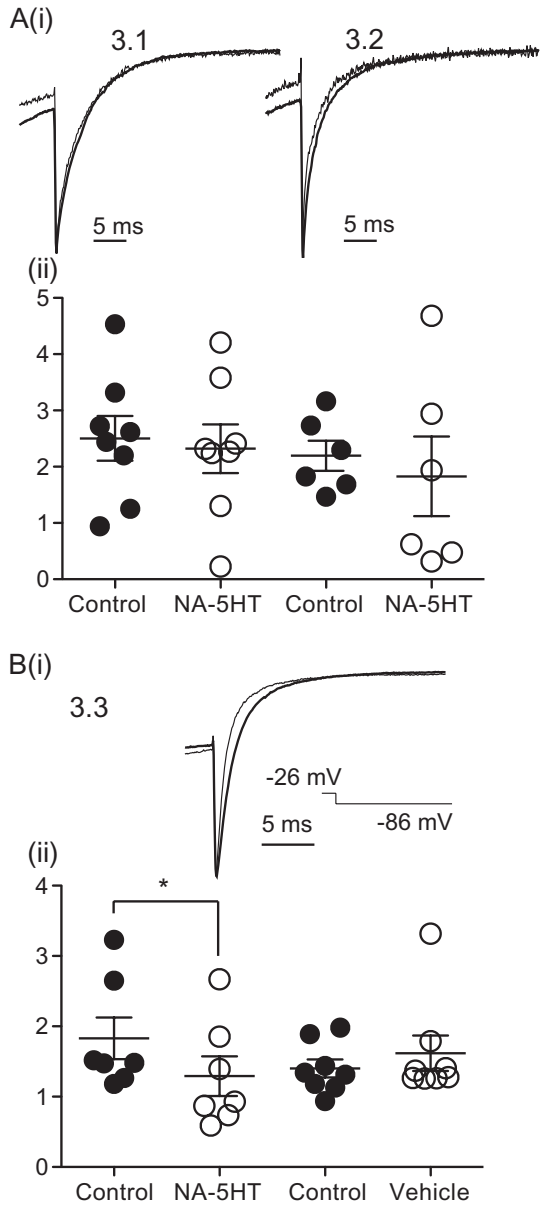

Figure 10

N-arachidonoyl 5-HT selectively affects $Ca_V3.3$ channel deactivation. Whole-cell patch clamp recordings were made from human $Ca_V3.1$, $Ca_V3.2$ and $Ca_V3.3$ channels stably expressed in HEK 293 cells. Currents were evoked by stepping cells repetitively from –86 to –26 mV every 10 s and tail current kinetics measured by fitting to a two-component exponential curve in Axograph. (A) Effects of NA-5HT (1 μM) on $Ca_V3.1$ and $Ca_V3.2$ tail currents. (i) Example traces of tail currents before and during NA-5HT application. (ii) τ for the major component of decay before and during NA-5HT superfusion. The bars are the mean ± SEM of at least six cells per condition. There were no differences in the τ for decay for $Ca_V3.2$ and $Ca_V3.3$ in the presence and absence of NA-5HT (paired *t*-test). (B) Effects of NA-5HT (1 μM) on $Ca_V3.3$ tail currents. (i) Example traces of tail currents before and during NA-5HT application. (ii) The τ for the major component of decay before and during NA-5HT superfusion and in vehicle controls. The bars are the mean ± SEM of at least six cells per condition. There was a significant difference in the τ for decay for $Ca_V3.3$ during NA-5HT superfusion. $^*P < 0.05$, Student's paired *t*-test.

2006). The expression of Ca_V3 channels in C6 or K-ras-transformed rat thyroid cells is incompletely characterized (Bertolesi *et al.*, 2002); however, it is tempting to speculate that the effects of NA-5HT on growth of these cells may be mediated via inhibition of T-type calcium channels.

The effects of NA-5HT Ca_V3 channels are quite similar to that of other NAAN such as NA-DA, NA-Gly and NA-GABA-OH (Barbara *et al.*, 2009; Ross *et al.*, 2009). All four compounds produce strong hyperpolarizing shifts in the membrane potential at which Ca_V3 channels inactivate, which would have the effect of reducing the number of channels available to open from all but the most negative membrane potentials. This mechanism for modulation of Ca_V3 is shared with arachidonic acid (Zhang *et al.*, 2000; Talavera *et al.*, 2004; Chemin *et al.*, 2007) and the phytocannabinoids Δ^9-tetrahydrocannabinol and cannabidiol (Ross *et al.*, 2008). In addition to effects on steady-state channel inactivation, anandamide and arachidonic acid both have effects on the kinetics of Ca_V3 channels, manifest by an acceleration of channel opening and open state inactivation, although the effects of AEA on $Ca_V3.2$ kinetics only occur at quite high concentrations (Chemin *et al.*, 2001; 2007; Talavera *et al.*, 2004). These kinetic effects are absent or minimal with NA-Gly and NA-DA modulation of Ca_V3 channels (Ross *et al.*, 2009), and NA-5HT did not affect the channel opening or open state inactivation of $Ca_V3.1$ and $Ca_V3.2$ in the present study. However, NA-5HT accelerated the apparent activation, inactivation from an open state and deactivation of $Ca_V3.3$. In the presence of NA-5HT, the kinetics of $Ca_V3.3$ activation were accelerated to a degree that approximates a 10 mV positive shift in membrane potential (Figure 8). This acceleration occurred in the absence of any significant effect on the voltage-dependence of channel activation, suggesting that NA-5HT may have affected a transition between open and inactivated state(s) of the channel. NA-5HT modulation of Ca_V3 channel kinetics resembles that of AEA in that the $Ca_V3.3$ channels are the most strongly affected, and neither drug dramatically affects $Ca_V3.2$ kinetics. The acceleration of entry into an inactivated state, coupled with an enhanced deactivation, would contribute to a reduction of calcium entry through any channels that opened in the presence of NA-5HT.

Ca_V3 subtype-specific effects have been observed with several modulators of the channels including Zn^{2+} and Δ^9-tetrahydrocannabinol (Traboulsie *et al.*, 2007; Ross *et al.*, 2008). In contrast to the effects of NA-5HT, Zn^{2+} selectively slows the inactivation from an open state and deactivation of $Ca_V3.3$, while Δ^9-tetrahydrocannabinol has similar effects to Zn^{2+} on $Ca_V3.1$ and $Ca_V3.2$ but not $Ca_V3.3$. It is tempting to speculate that these compounds act by modulating channel activity through common binding sites on the channels that have slightly different ligand recognition properties and which can speed *or* slow the transitions between different states of the channels. However, the site(s) of action for lipophilic ligand modulation of Ca_V3 channels is not known, and there is limited information about where any drugs that modulate Ca_V3 channels bind to affect channel function.

NA-5HT is an endogenous compound (Verhoeckx *et al.*, 2011), and it is regularly used as pharmacological probe for cannabinoid-related (patho)physiological processes. Our data suggest a novel role for NA-5HT as an endogenous

modulator of cellular excitability through its actions on T-type calcium channels, although confirmation of this awaits the development of selective inhibitors of NA-5HT metabolism or compounds that selectively affect the binding site(s) for NA-5HT on the channels.

Acknowledgements

This work was supported by National Health and Medical Research Council of Australia Project 1002680 to MC and MK. AG was supported by a University of Sydney postgraduate award and Kolling Institute award. AG, MH, AR, MK and MC performed experiments and analysed data. AG and MC wrote the paper.

Conflicts of interest

None.

References

Alexander SPH, Mathie A, Peters JA (2011). Guide to receptors and channels (GRAC), 5th edition. Br J Pharmacol 164 (Suppl. 1): S1–S324.

Barbara G, Alloui A, Nargeot J, Lory P, Eschalier A, Bourinet E *et al.* (2009). T-type calcium channel inhibition underlies the analgesic effects of the endogenous lipoamino acids. J Neurosci 29: 13106–13114.

Bertolesi GE, Shi C, Elbaum L, Jollimore C, Rozenberg G, Barnes S *et al.* (2002). The Ca^{2+} channel antagonists mibefradil and pimozide inhibit cell growth via different cytotoxic mechanisms. Mol Pharmacol 62: 210–219.

Bifulco M, Laezza C, Valenti M, Ligestri A, Portella G, Di Marzo V (2004). A new strategy to block tumor growth by inhibiting endocannabinoid inactivation. FASEB J 18: 1606–1608.

Bisogno T, Melck D, De Petrocellis L, Yu M, Bobrov MY, Gretskaya NM *et al.* (1998). Arachidonoylserotonin and other novel inhibitors of fatty acid amide hydrolase. Biochem Biophys Res Comm 248: 515–522.

Bisogno T, Melck D, Bobrov MY, Gretskaya NM, Bezuglov VV, De Petrocellis L *et al.* (2000). *N*-acyl-dopamines: novel synthetic CB_1 cannabinoid-receptor ligands and inhibitors of anandamide inactivation with cannabimimetic activity *in vitro* and *in vivo*. Biochem J 351: 817–824.

Bourinet E, Alloui A, Monteil A, Barrere C, Couette B, Poirot O *et al.* (2005). Silencing of the $Ca_V3.2$ T-type calcium channel gene in sensory neurons demonstrates its major role in nociception. EMBO J 24: 315–324.

Burstein SH, Rossetti RG, Yagen B, Zurier RB (2000). Oxidative metabolism of anandamide. Prostaglandins Other Lipid Mediat 61: 29–41.

Chemin J, Monteil A, Perez-Reyes E, Nargeot J, Lory P (2001). Direct inhibition of T-type calcium channels by the endogenous cannabinoid anandamide. EMBO J 20: 7033–7040.

Chemin J, Nargeot J, Lory P (2007). Chemical determinants involved in anandamide-induced inhibition of T-type calcium channels. J Biol Chem 282: 2314–2323.

Connor M, Vaughan CW, Vandenberg R (2010). *N*-Acyl amino acids and *N*-acyl neurotransmitter conjugates: neuromodulators and probes for new drug targets. Br J Pharmacol 160: 1857–1871.

Costa B, Bettoni I, Petrosino S, Comelli F, Giagnoni G, Di Marzo V (2010). The dual fatty acid amide hydrolase/TRPV1 blocker, *N*-arachidonoyl-serotonin, relieves carrageenan-induced inflammation and hyperalgesia in mice. Pharm Res 61: 537–546.

Cribbs LL, Lee JH, Yang J, Satin J, Zhang Y, Daud A *et al.* (1998). Cloning and characterization of alpha1H from human heart, a member of the T-type Ca^{2+} channel gene family. Circ Res 83: 103–109.

Cribbs LL, Gomora JC, Daud AN, Lee JH, Perez-Reyes E (2000). Molecular cloning and functional expression of $Ca_V3.1c$, a T-type calcium channel from human brain. FEBS Lett 466: 54–58.

D'Argenio G, Valenti M, Scaglione G, Cosenza V, Sorrentini I, Di Marzo V (2006). Up-regulation of anandamide levels as an endogenous mechanism and a pharmacological strategy to limit colon inflammation. FASEB J 20: 568–570.

Di Marzo V, Capasso R, Matias I, Aviello G, Petrosino S, Borrelli F *et al.* (2008). The role of endocannabinoids in the regulation of gastric emptying: alterations in mice fed a high fat diet. Br J Pharmacol 153: 1271–1280.

Docherty RJ, Yeats JC, Piper AC (1997). Capsazepine block of voltage-activated calcium channels in adult dorsal root ganglion neurones in culture. Br J Pharmacol 121: 1461–1467.

Edington AR, McKinzie AA, Reynolds AJ, Kassiou M, Ryan RM, Vandenberg RJ (2009). Extracellular loops 2 and 4 of GLYT2 are required for N-arachidonyl-glycine inhibition of glycine transport. J Biol Chem 284: 36424–36430.

Fowler CJ, Tiger G, Lopez-Rodriguez ML, Viso A, Ortega-Gutierrez S, Ramos JA (2003). Inhibition of fatty acid aminohydrolase, the enzyme responsible for the metabolism of the endocannabinoid anandamide, by analogs of arachidonoyl-serotonin. J Enzyme Inhib Med Chem 18: 225–231.

Frazier CJ, Serrano JR, George EG, Yu X, Viswanathan A, Perez-Reyes E *et al.* (2001). Gating kinetics of the α1I T-type calcium channel. J Gen Physiol 118: 457–470.

Giordanetto F, Knerr L, Wallberg A (2011). T-type calcium channel inhibitors: a patent review. Expert Opin Ther Patents 21: 85–191.

Gomora JC, Murbartian J, Arias JM, Lee J-H, Perez-Reyes E (2002). Cloning and expression of the human T-type channel $Ca_V3.3$: insights into prepulse facilitation. Biophys J 83: 229–241.

Guo J, Williams DJ, Ikeda SR (2008). *N*-arachidonyl serine, a putative endocannabinoid, alters the activation of N-type calcium channels in sympathetic neurons. J Neurophysiol 100: 1147–1151.

Hamill OP, Marty A, Neher E, Sakmann B, Sigworth FJ (1981). Improved patch-clamp techniques for high-resolution current recording from cells and cell-free membrane patches. Pflugers Arch 391: 85–100.

Heblinski M, Connor M (2012). Agonist regulation of 5HT1B receptor signaling. Proc 32nd Aust Neurosci Soc, p 77.

Huang SM, Bisogno T, Petros TJ, Chang S-Y, Zavitsanos PA, Zipkin RE *et al.* (2001). Identification of a new class of molecules, the arachidonyl amino acids, and characterization of one member that inhibits pain. J Biol Chem 276: 42639–42634.

Huang SM, Bisogno T, Trevisani M, Al-Hayani A, de Petrocellis L, Fezza F *et al*. (2002). An endogenous capsaicin-like substance with high potency at recombinant and native vanilloid receptors. Proc Natl Acad Sci U S A 99: 8400–8405.

Jacobsson SOP, Wallin T, Fowler CJ (2001). Inhibition of rat C6 glioma cell proliferation by endogenous and synthetic cannabinoids. Relative involvement of cannabinoid and vanilloid receptors. J Pharmacol Exp Ther 299: 951–959.

Jonsson K-O, Vandevoorde S, Lambert DM, Tiger G, Fowler CJ (2001). Effects of homologs and analogs of palmitoylethanolamide upon the inactivation of the endocannabinoid anandamide. Br J Pharmacol 133: 1263–1275.

Kim D, Park D, Choi S, Lee S, Sun M, Kim C *et al*. (2003). Thalamic control of visceral nociception mediated by T-type calcium channels. Science 302: 117–119.

Maione S, de Petrocellis L, de Novellis V, Schiano Moriello A, Petrosino S, Palazzo E *et al*. (2007). Analgesic actions of *N*-arachidonoyl-serotonin, a fatty acid amide hydrolase inhibitor with antagonistic activity at vanilloid TRPV1 receptors. Br J Pharmacol 150: 766–781.

Marinelli S, Di Marzo V, Florenzano F, Fezza F, Viscomi MT, van der Stelt M *et al*. (2007). *N*-arachidonoyl-dopamine tunes synaptic transmission onto dopaminergic neurons by activating both cannabinoid and vanilloid receptors. Neuropsychopharmacology 32: 298–308.

de Novellis V, Palazzo E, Rossi F, De Petrocellis L, Petrosino S, Guida F *et al*. (2008). The analgesic effect of N-arachidonoyl-serotonin, a FAAH inhibitor and TRPV1 receptor antagonist, associated with changes in rostral ventromedial medulla and locus coeruleus cell activity in rats. Neuropharmacology 55: 1105–1113.

de Novellis V, Vita D, Gatta L, Luongo L, Bellini G, De Chiaro M *et al*. (2011). The blockade of the transient receptor potential type 1 and fatty amide hydrolase decreases symptoms and central sequelae in the medial prefrontal cortex of neuropathic rats. Mol Pain 7: 7.

Panner A, Wurster RD (2006). T-type calcium channels and tumor proliferation. Cell Calcium 40: 253–259.

Park C, Kim JH, Yoon BE, Choi EJ, Lee CJ, Shin HS (2010). T-type channels control the opioidergic descending analgesia at the low threshold-spiking GABAergic neurons in the periaqueductal gray. Proc Natl Acad Sci U S A 107: 14857–14862.

Perez-Reyes E (2003). Molecular physiology of low-voltage-activated T-type calcium channels. Physiol Rev 83: 117–161.

Ross HR, Napier I, Connor M (2008). Inhibition of recombinant human T-type calcium channels by Δ^9-Tetrahydrocannabinol and cannabidiol. J Biol Chem 283: 16124–16134.

Ross HR, Gilmore AJ, Connor M (2009). Inhibition of human recombinant T-type calcium channels by the endocannabinoid arachidonyl dopamine. Br J Pharm 156: 740–750.

Shin H-S, Cheong E-J, Choi S, Lee J, Na HS (2008). T-type calcium channels as therapeutic targets in the nervous system. Curr Opin Pharmacol 8: 33–41.

Succar R, Mitchell VA, Vaughan CW (2007). Actions of *N*-arachidonyl-glycine in a rat inflammatory pain model. Mol Pain 3: 24.

Suplita RL II, Farthing JN, Gutierrez T, Hohmann AG (2005). Inhibition of fatty-acid amide hydrolase enhances cannabinoid stress-induced analgesia: sites of action in the dorsal periaqueductal grey and rostral ventromedial medulla. Neuropharmacology 49: 1201–1209.

Suplita RL II, Gutierrez T, Fegley D, Piomelli D, Hohmann AG (2006). Endocannabinoids at the spinal level regulate, but do not mediate, nonopioid stress-induced analgesia. Neuropharmacology 50: 372–379.

Talavera K, Staes M, Janssens A, Droogmans G, Nilius B (2004). Mechanism of arachidonic acid modulation of the T-type calcium channel α_{1g}. J Gen Physiol 124: 225–238.

Traboulsie A, Chemin J, Chevalier M, Quignard J-F, Nargeot J, Lory P (2007). Subunit-specific modulation of T-type calcium channels by zinc. J Physiol 578: 159–171.

Verhoeckx KCM, Voortman T, Balvers MGJ, Hendriks HFJ, Wortelboer HM, Witkamp RF (2011). Presence formation and putative biological activities of N-acyl serotonins, a novel class of fatty-acid derived mediators, in the intestinal tract. Biochem Biophys Acta 1811: 578–586.

Vuong LAQ, Mitchell VA, Vaughan CW (2008). Actions of *N*-arachidonyl-glycine in a rat neuropathic pain model. Neuropharmacology 54: 189–193.

Wiles AL, Pearlman RJ, Rosvall M, Aubrey K, Vandenberg RJ (2006). *N*-arachidonyl glycine inhibits the glycine transporter, GLYT2a. J Neurochem 99: 781–786.

Yang Z, Aubrey KR, Alroy I, Harvey RJ, Vandenberg RJ, Lynch JW (2008). Subunit-specific modulation of glycine receptors by cannabinoids and *N*-arachidonyl-glycine. Biochem Pharmacol 76: 1014–1023.

Yevenes GE, Zeilhofer HU (2011). Molecular sites for the positive allosteric modulation of glycine receptors by endocannabinoids. PLoS ONE 6: e23886.

Zhang Y, Cribbs L, Satin J (2000). Arachidonic acid modulation of α1H, a cloned human T-type calcium channel. Am J Physiol Heart Circ Physiol 278: H184–H193.